

# The weldability of AZ31 magnesium alloy by friction stir welding

M. Aydin<sup>1,2\*</sup>, R. Bulut<sup>2</sup>

<sup>1</sup>*Southern Illinois University at Carbondale, Department of Mechanical Engineering and Energy Process, Carbondale, IL 62901 USA*

<sup>2</sup>*Dumlupinar University, Department of Mechanical Engineering, Main Campus, 43100 Kutahya, Turkey*

Received 30 September 2009, received in revised form 20 October 2009, accepted 22 October 2009

## Abstract

Friction stir welding is a relatively new joining technique particularly for aluminium and magnesium alloys that are difficult to join with fusion welding methods. In this study, rolled AZ31 magnesium alloy was joined by friction stir welding method in 960, 1964 and 2880 rpm rotational speeds and in 10 and 20 mm min<sup>-1</sup> transverse speeds. During the welding process, due to the low temperature occurring in low rotations, a coarser surface was obtained. Thanks to the microstructural refinement, the hardness of the stir zone was observed lower compared with the hardness of the parent material due to the temperature released by friction. The fractures mostly occurred at the heat affected zone. The maximum tensile strength of joint reached 93 % of that of base materials, at the 1964 rpm rotational speed and 20 mm min<sup>-1</sup> transverse speed.

**Key words:** magnesium alloys, hardness, scanning electron microscopy, friction stir welding

## 1. Introduction

Magnesium alloys possess such characteristics as low density, high specific resistance, weldability, castability, recycling, and abundance [1]. This is why magnesium alloy practices will rapidly improve in near future, and it is foreseen that it will increase especially in automotive and transportation sectors [2, 3]. Today, magnesium alloy parts are commonly manufactured in casts, and its manufacturing by plastic moulding-rolling and welding is quite limited. Due to these limitations, the application areas of magnesium (Mg) alloys are unable to develop. An effective and inexpensive manufacturing or joining method would develop the industrial utilisation of these materials. The welding is an effective and cheap method of industrial applications, and it can be applied on numerous metallic materials. Friction stir welding (FSW) is a solid-state welding method invented in 1991 (British TWI) [4–7]. When compared with traditional welding methods, this one bears various advantages. These do not necessitate protective gas, additional wiring, and personal

protective measures and are eco-friendly. Such negativities as porosity formation, gas cavities, inclusions, etc. on the welding are not observed. This method began to be applied on aluminium alloys [6, 8–11] and, in recent years, on magnesium alloys. Studies were reported specifically on AZ alloys (Mg-Al-Zn) and AM (Mg-Al-Mn) [4, 12–14]. However, studies conducted on AZ alloys are far from being sufficient. AZ alloys were reported to produce better mechanical characteristics compared with friction stir welding and TIG welding [7, 15]. Satoshi et al. [14] reported a lower hardness and smaller grain size in the weld zone of AZ31 magnesium alloy compared to the base metal. In addition, even though there are many studies on friction stir welding, there still exists a need to study its effects on surface quality, temperature change, mechanical properties and microstructure. Additionally, the relationship between the welding parameters and mechanical and microstructural characteristics in friction stir welding has not yet been properly understood. Determination of right parameters and their optimisation is of necessity.

\*Corresponding author: tel.: +1 618 453 3680, +902742652031; fax: +1 618 453 7658; e-mail address: [maydin@engr.siu.edu](mailto:maydin@engr.siu.edu), [m\\_aydin@dumlupinar.edu.tr](mailto:m_aydin@dumlupinar.edu.tr)

Table 1. The chemical composition (vol.%) of the AZ31 magnesium alloy from present study

Al	Zn	Mn (min)	Co (max)	Si (max)	Cu (max)	Ni (max)	Fe (max)	Other (max)
2.5–3.5	0.6–1.4	0.20	0.04	0.10	0.05	0.05	0.005	0.30

Table 2. The selected properties of the AZ31 magnesium alloy from literature and the present study

Specimen (Base metal)	Yield strength (MPa)	Ultimate strength (MPa)	Elongation (%)	Hardness, HV
AZ31(Literature )	~ 122	275 [4], 208 [5], 250 [17]	16	55–72
AZ31 (Present study)	97	197	4	82

Table 3. Welding parameters selected in the present study for the friction stir welding of AZ31 magnesium alloy butt joints

Sample No	Rotational speed (rpm)	Welding speed (mm min <sup>-1</sup> )
A1.1	960	10
A1.2	960	20
A2.1	1964	10
A2.2	1964	20
A3.1	2880	10
A3.2	2880	20

## 2. Experimental studies

AZ31 rolled magnesium alloy plate materials were utilised in this study. The composition of this alloy is given in Table 1 and some of its significant characteristics are shown in Table 2. Samples were cut in 120 × 150 mm<sup>2</sup> size of 4 mm thickness, placed in the milling machine, and then joined through the welding parameters given in Table 3. At the time of welding, the rotational speeds of friction stir pins in the milling machine were measured by utilising type laser device. The changes of temperature during the welding process were measured with K-type thermocouple and laser device for each cm. The temperatures measured were recorded and used as a data to draw graphs.

The pins used for the friction stir welding were manufactured from 2344 H13 tool steel of which the photograph is shown in Fig. 1. The welding pins have shoulder and pin. The diameter of shoulder and pin is 20 mm and M4, respectively. The length of pin is 3.8 mm. The hardness of pins was brought to 57 HRC through heat treatment. Joining procedure was performed by binding the samples to the plate of the universal milling machine and in different speeds and rotations of parameters given in Table 3.

Single pass welding procedure was used to fabric-



Fig. 1. The photograph of welding pin utilised in experiments dimensions.

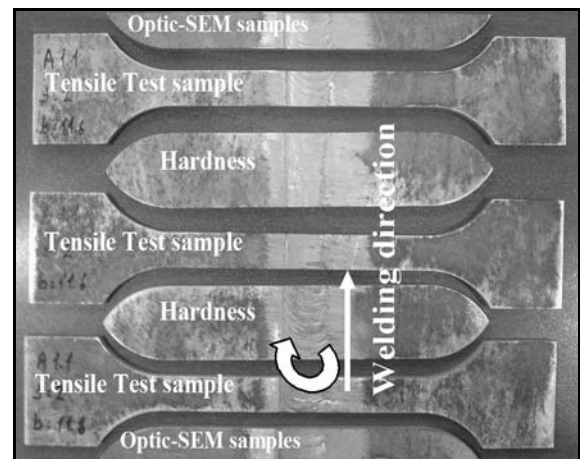


Fig. 2. Extraction of experimental samples from welded samples cut by wire erosion.

ate the joints. Three welded samples were obtained for each parameter. As seen in Fig. 2, three tensile samples, two microhardness, and two optic-SEM mi-

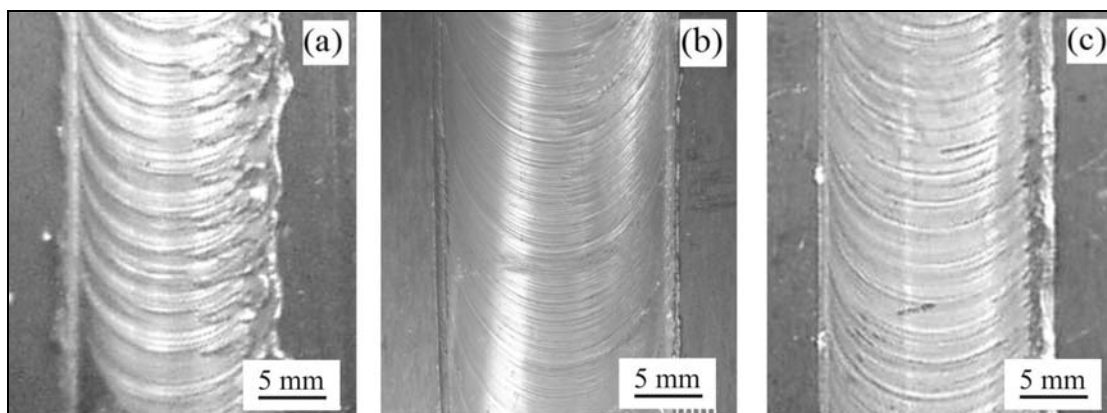


Fig. 3. The surface illustrates different rotational speed and welding speed parameters of welded samples: a) 960 rpm,  $10 \text{ mm min}^{-1}$  (A1.1), b) 1964 rpm,  $20 \text{ mm min}^{-1}$  (A2.2), c) 2880 rpm,  $10 \text{ mm min}^{-1}$  (A3.1).

cross-section samples conforming to EN 895 standards were extracted from each  $240 \times 150 \text{ mm}^2$  welded joint by precisely cutting through wire erosion method.

Following the obtaining of optical and SEM specimens vertically to the cross-section of samples extracted by cutting via wire erosion method, mechanical grinding and polishing processes were carried out. After being mechanically ground and polished, specimens were etched with 5 g picric acid + 5 ml acetic acid + 10 ml water + 100 ml ethanol reagent to reveal the macrostructure and microstructure [4, 16–18]. Final polishing was done using the diamond compound  $0.03 \mu\text{m}$  particle size in the disc-polishing machine. Macrostructure and microstructure analyses were carried out using a light optical microscopy-Shimadzu 2000 and JEOL 6060 scanning electron microscopy. Tensile tests were performed by Shimadzu AG-IS, Autograph device at  $4 \text{ mm min}^{-1}$  tensile speed. Vickers hardness test was conducted using a 200 gf load for 10 s as Lee et al. [17] and Darras et al. [19] with Digital microhardness tester HVL 1000 test machine. In this paper, the effect of the transverse and rotational speed on the surface roughness, microstructure, and mechanical properties was studied.

### 3. Results and discussion

#### 3.1. Effect of process parameters on weld formation

The roughness of welded surfaces could not be measured with surface roughness device since welded surfaces obtained were very coarse. So the roughness of welded surfaces was detected visually. Figure 3 shows the surface views of plates joined by FSW. The sample shown in Fig. 3a, which was obtained under 960 rpm, has large defect with valley-like structures formed in the friction stir welded zone (SZ) with a very rough surface. Defect-free welds were successfully obtained in

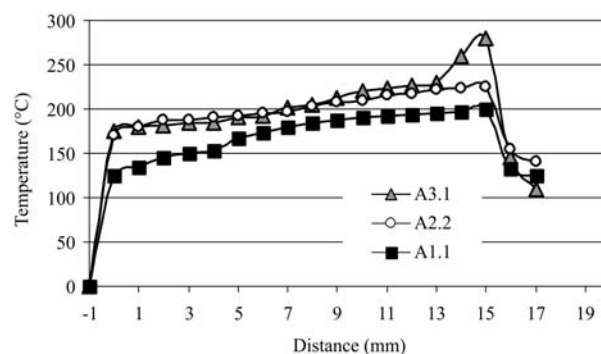


Fig. 4. The changes of temperature with different welding parameters during the friction stir welding of AZ31 Mg alloy.

Fig. 3b with 1964 rpm and in Fig. 3c with 2880 rpm samples. In addition, the surface morphology of the SZ became smoother with an increase in the tool rotational speed. These results demonstrate the presence of optimum tool rotation and progress speed in order to obtain the AZ31 magnesium alloy as a defect-free joining [11]. Gharacheh et al. [10] obtained full penetration welds in nugget zone at 1400/20 rotational speed/transverse speed compared to 650/50 rotational speed/transverse speed. In this study, it was observed in macro photographs that the depth of welded stir zone and surface smoothness improved and a total permeable joining zone (Fig. 5) was obtained when the rotational speed and progress speed of the tool was increased. In these joints, the best joining is seen in Figs. 3b and 5a, which were obtained with 1964 rpm rotational speed and  $20 \text{ mm min}^{-1}$  transverse speed.

A deeper and smoother joining was obtained thanks to the heat input formed by an increase in the rotational speed at the time of welding. To put it another way, the heat of welding metal increases with increase in rotation/transverse speed rate [12].

Figure 4 shows the heat changes measured dur-

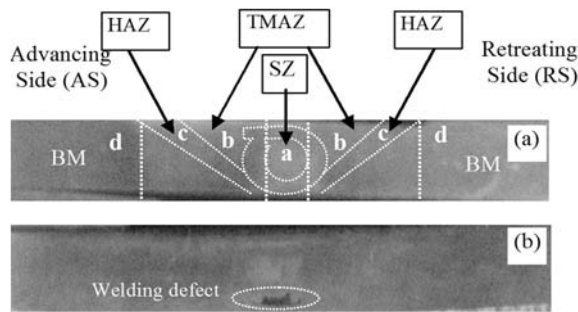


Fig. 5. Transverse section of the two welded rolling plates of AZ31: a) 1964 rpm – 20 mm min<sup>-1</sup> and b) 960 rpm – 10 mm min<sup>-1</sup>.

ing the welding process. The graph demonstrates that, among the welded specimens, a sufficient heat could not be obtained in A1.1, and a higher heat was acquired in A3.1. However, as it can also be seen in Fig. 3, there was sporadic cracking and spinning parallel to a heat increase. In addition, as shown in the heat graph, the specimen A2.2 had the heat necessary for sufficient softening and a smoother surface was acquired.

Figure 5 shows the typical cross-sectional macrographs of FSWed AZ31 Mg alloys. In Fig. 5a, no welding defect was detected in the joint, indicating that the FSW AZ31 Mg alloy joint can be achieved under investigated welding parameter (rotational speed of 1964 and transverse speed of 20 mm min<sup>-1</sup>). But Fig. 5b shows welding defect was detected at the bottom of the plate under investigated welding parameter (rotational speed of 960 rpm and transverse speed of 10 mm min<sup>-1</sup>). As identified in FSW aluminium alloys [1, 12], three microstructural zones were nugget zone (NZ), thermomechanically affected zone (TMAZ) and heat-affected zone (HAZ). The nugget zone exhibited

a basin-like shape, which was similar to that observed in FSW AZ31 [13]. Figure 5 shows typical optical micrographs of (a) SZ, (b) TMAZ, (c) HAZ and (d) base metal corresponding to the zones marked in Fig. 5a.

### 3.2. Microstructures

Figure 6 shows the cross-sectional scanning electron microstructure (SEM) of FSWed AZ31 Mg alloys. In Fig. 6a, no welding defect was detected in the joint, indicating that the FSW AZ31 Mg alloy joint can be achieved under investigated welding parameter (rotational speed of 1964 and transverse speed of 20 mm min<sup>-1</sup>). Figure 6b shows the porosity and crack of the welded sample under the welding parameter (rotational speed of 960 rpm and transverse speed of 10 mm min<sup>-1</sup>). As seen in Figs. 5b and 6b, there were porosities and cavities and cracks in upper zones caused by spinning in low rotations in both optic and SEM microstructures. The reason for this is the inability to constitute softening, thus, infusion due to the fact that enough heat could not be produced in lower rotations and transverse speeds.

In Fig. 7, the parent material exhibited a typical as-rolled structure, characterised by coarse strip-like structures and large secondary phase particles with the fine dynamic recrystallized grains being distributed between coarse strip-like structures (Fig. 7a). The elongated grains in the base metal have become equiaxed and recrystallized in the stir zone during welding process. Besides, at the transition zone between thermomechanically affected zone and stir zone grains are in general equiaxed. The evaluation of recrystallized grain structure in the stir zone is due to the severe plastic deformation and frictional heat produced by the rotating tool pin and its shoulder in the stir zone during welding. Intense plastic deformation and frictional heating during FSW resulted in the gen-

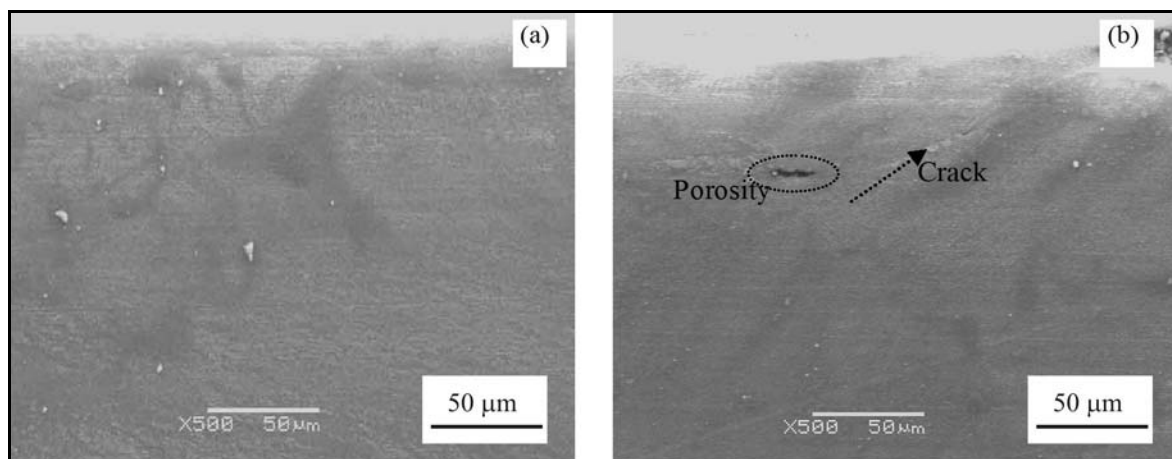


Fig. 6. The SEM microstructures of the transverse section of the welded two rolling plates of AZ31: a) 1964 rpm – 20 mm min<sup>-1</sup> and b) 960 rpm – 10 mm min<sup>-1</sup>.

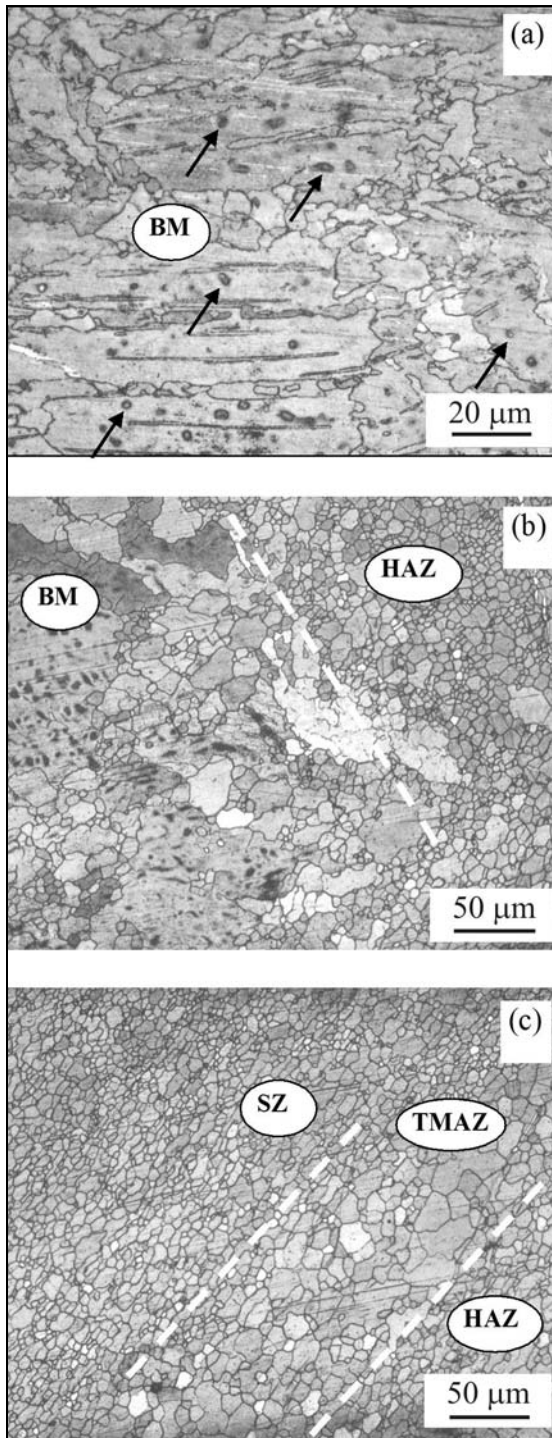


Fig. 7. Typical optical microstructures of a) AZ31 based material, b) transition zone of BM/HAZ, and c) transition zones of SZ/TMAZ/HAZ.

eration of fine recrystallized grains within the nugget zone (NZ) (Fig. 7b,c). Similar observations have been made in FSW AZ31B and Mg-Zn-Y-Zr alloy [5, 18]. The grain size of NZ was significantly smaller than that of the parent material. The smaller grains pro-

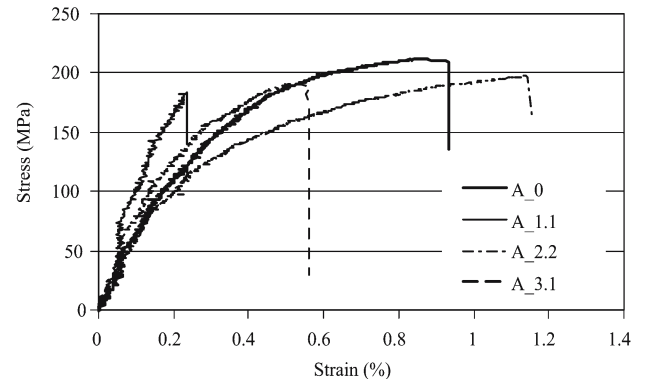


Fig. 8. The stress-strain graphs of the different parameter welded samples.

duced in the stir zone induced by the faster welding speed are attributed to the relative lower heat input in the weld [5]. The grain size in HAZ was coarser than that in the NZ with the precipitates being coarsened and/or dissolved into the matrix. Therefore, the HAZ was usually the weakest zone of FSWed joint [18]. Darnas et al. [19] stated that, in this area, the finer and more homogeneous grain structure produced by FSW is expected to improve the ductility and formability of the materials. Figure 7c shows the interface between the TMAZ and SZ. In the TMAZ, the dynamic recrystallization did not occur due to insufficient deformation strain and thermal exposure, and the elongated grains with coarse secondary phase particles being distributed along flow line were observed (Fig. 7c).

### 3.3. Tensile test results

Figure 8 shows the tensile test results for specimens having different rotational speeds and different welding speeds. The base materials show a 210 MPa tensile strength, which is consistent with the literature [4, 5, 12, 17]. Figure 8 shows that the FSW joint exhibited somewhat decreased ultimate tensile strength when compared to the parent materials. As shown in Fig. 8, the maximum tensile strength of 197 MPa, obtained at a rotation speed of 1964 rpm and a welding speed of  $20 \text{ mm min}^{-1}$ , was 93 % of that of the base material. Similar results were reported by Xie et al. [18] and Zhang et al. [1], 95 % and 91 %, respectively. Notwithstanding, the lowest tensile resistance was obtained from the sample coded as A1.1 via 960 rpm and  $10 \text{ mm min}^{-1}$  due to the tunnel defect and porosities (Figs. 5 and 6), which resulted in poor properties of the joints. This shows that the welding parameters were effective on joining resistance in the welding process of AZ31 alloy, and that a rotation and progress speed need to be ascertained. A sufficient friction heat did not come out in lower rotation and transverse speeds in the sample coded A1.1, and as seen in

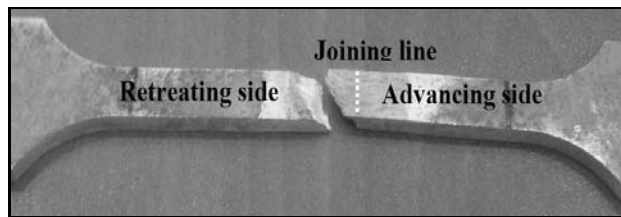


Fig. 9. The macrographs of the fractured sample at the 1964 rpm and  $20 \text{ mm min}^{-1}$  conditions welded sample.

tensile test graph (Fig. 8), a brittle structure was not formed. Thus, it produced a lower tensile resistance value. Although the tensile resistance was higher in high rotations and progress speeds in the sample coded A3.2 compared with the one coded A1.1, it gave lower tensile resistance than the sample A2.2. The reason is, as known, that the lower rotational speed creates smaller weld zone due to the lower heat input. The reason for such a decrease in the tensile properties could be explained by the grain growth in the boundary between the TMAZ and the stir zone at advanced side (AS), as reported by Lim et al. [20] and Gharacheh et al. [10]. Another reason would be as follows: Magnesium alloys having hcp crystal structure are responsible for this reduction in the tensile properties due to the formation of new crystallographic texture in the weld zone as reported by Park et al. [21].

The tensile test results showed that fracture locations were observed to be about 5–8 mm from the weld centre-line measured at the top surface of the specimens (Fig. 9). The fracture occurred in the HAZ on the retreating side, which was consistent with the lowest hardness distribution in the HAZ. During the FSW, the lower rotational speed creates smaller weld zone due to the lower heat input, and the boundary between the TMAZ and the SZ is as reported by Zhang et al. [2].

### 3.4. Microhardness

Figure 10 shows a typical hardness profile of a specimen (welding parameters  $1964 \text{ rpm}$ ,  $20 \text{ mm min}^{-1}$ ) across the weld zone at the top surface, 2.5 mm from the bottom surface. The left part of the hardness profile is on the AS and the right part is on the retreating side (RS). The results show that the average hardness value of weld was lower than that of base materials. The minimum hardness value appears near the SZ, and there exists a peak value near the HAZ as reported by Zhang et al. [1]. In average, the hardness of A1.1 sample is higher compared to the A2.2 and A3.1 samples. The reason for this is the lower temperature produced during the friction stir. Similar result was also observed in Denquin et al. [22]. Vilace et al. [23] reported that if the ratio of the rotational speed

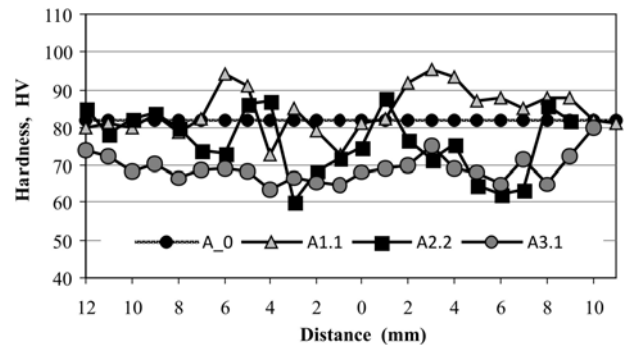


Fig. 10. Hardness profile of FSWed AZ31 alloy with different welding parameters.

(rpm) to the transverse speed ( $\text{mm min}^{-1}$ ) became more than  $4 \text{ mm min}^{-1}$ , it can be considered as a hot welding condition and the resulting hardness exhibits a lower value between TMAZ and HAZ. The hardness drop at the stir zone is due to the fact that there is a high temperature at that zone and the peak temperature reached is enough to soften the material in the nugget zone. The result is consistent with previously reported results for different magnesium [1, 5, 18] and aluminium alloys [24, 25]. The average HV values of SZ and BM are 73 and 82, respectively. The effect of rotational speed on the resulting hardness is shown in Fig. 10, which indicates that increasing the rotational speed tends to decrease the resulting hardness. This result is also consistent with the reported results for different magnesium [1, 5, 20, 21] and aluminium alloys [24–26].

## 4. Conclusion

1. The preliminary results on FSW of AZ31 Mg alloy are promising; grain refinement and homogenisation of the microstructure are achieved with a single pass process.
2. Under a rotation speed of  $1964 \text{ rpm}$  and a transverse speed of  $20 \text{ mm min}^{-1}$ , 4 mm thick rolled Mg-Al-Zn alloy plate was friction stir welded and defect-free weld with basin-like nugget zone was successfully obtained.
3. The surface morphology of the SZ became smoother with an increase in the rotational speed.
4. The weld zone was divided into three regions – SZ, TMAZ and HAZ – based on the microstructure. The SZ had fine and equiaxed grains because of dynamic recrystallization. Compared with the BM, Mg alloy grains in SZ were greatly refined because of dynamic recrystallization during friction stir welding process.
5. Microstructural examinations of AZ31 alloy after friction stir welding revealed that smaller grain

sizes were observed in the stir zone at a higher welding speed due to a higher heat input, because faster rotational speed and welding speed produce higher temperature in the stir zone.

6. The strengths of the FSW joint were only slightly lower than those at the parent material. The joining efficiency was as high as 93 %.

### Acknowledgements

This work is supported by the Council of Scientific Research Projects of Dumlupinar University (DPU-BAP-2008-06) of Turkey.

### References

- [1] ZHANG, B.—YUAN, S.—WANG, X.: *Rare Metals*, 27, 2008, p. 393. [doi:10.1016/S1001-0521\(08\)60151-5](https://doi.org/10.1016/S1001-0521(08)60151-5)
- [2] DATONG, Z.—MAYUMI, S.—KOUICHI, M.: *Scripta Materialia*, 52, 2005, p. 899.
- [3] AFRIN, N.—CHEN, D. L.—CAO, X.—JAHAZI, M.: *Materials Science and Engineering A*, 472, 2008, p. 179. [doi:10.1016/j.msea.2007.03.018](https://doi.org/10.1016/j.msea.2007.03.018)
- [4] WANG, X.—WANG, K.: *Materials Science and Engineering A*, 431, 2006, p. 114.
- [5] HWANG, Y. M.—KANG, Z. W.—CHIOU, Y. C.—HSU, H. H.: *International Journal of Machine Tools and Manufacture*. [doi:10.1016/j.ijmactools.2007.12.003](https://doi.org/10.1016/j.ijmactools.2007.12.003)
- [6] AMANCIO FILHO, S. T.—SHEIKHI, S.—DOS SANTOS, J. F.—BOLFARINI, C.: *Journal of Materials Processing Technology*. [doi:10.1016/j.imatprotec.2007.12.008](https://doi.org/10.1016/j.imatprotec.2007.12.008)
- [7] BALASUBRAMANIAN, V.: *Materials Science and Engineering A*, 480, 2008, p. 397.
- [8] LIU, P.—SHI, Q.—WANG, W.—WANG, X.—ZHANG, Z.: *Materials Letters*, 62, 2008, p. 4106. [doi:10.1016/j.matlet.2008.06.004](https://doi.org/10.1016/j.matlet.2008.06.004)
- [9] KWON, Y. J.—SHIGEMATSU, I.—SAITO, N.: *Materials Letters*, 62, 2008, p. 3827. [doi:10.1016/j.matlet.2008.04.080](https://doi.org/10.1016/j.matlet.2008.04.080)
- [10] GHARACHEH, M. A.—KOKABI, A. H.—DANESHI, G. H.—SHALCHI, B.—SARRAFI, R.: *International Journal of Machine Tools and Manufacture*, 46, 2006, p. 1983.
- [11] LI, N.—PAN, T. Y.—COOPER, R. P.—HOUSTON, D. Q.—FENG, Z.—SANTELLA, M. L.: *Magnesium Technology*. Ed.: Lou, A. TMS (The Minerals, Metals and Materials Society) 2004.
- [12] PARK, S. H. C.—SATO, Y. S.—KOKAWA, H.: *Scripta Materialia*, 49, 2003, p. 161. [doi:10.1016/S1359-6462\(03\)00210-0](https://doi.org/10.1016/S1359-6462(03)00210-0)
- [13] NAKATA, K.—KIM, Y. G.—USHIO, M.: *Trans JWRJ*, 31, 2002, p. 141.
- [14] SATOSHI, H.—KAZUTAKA, O.—MASAYUKI, D.—HISANORI, O.—MASAHISA, I.—YASUHISA, A. Q.: *J. Jpn. Weld Soc.*, 21, 2003, p. 539.
- [15] WOO, W.—CHOO, H.—BROWN, D. W.—LIAW, P. K.—FENG, Z.: *Scripta Materialia*, 54, 2006, p. 1859. [doi:10.1016/j.scriptamat.2006.02.019](https://doi.org/10.1016/j.scriptamat.2006.02.019)
- [16] ZHANG, H.—WU, H.—HUANG, J.—SANBAO, L.—WU, L.: *Rare Metals*, 26, 2007, p. 158. [doi:10.1016/S1001-0521\(07\)60177-6](https://doi.org/10.1016/S1001-0521(07)60177-6)
- [17] LEE, C. J.—HUANG, J. C.—HSIEH, P. J.: *Scripta Materialia*, 54, 2006, p. 1415. [doi:10.1016/j.scriptamat.2005.11.056](https://doi.org/10.1016/j.scriptamat.2005.11.056)
- [18] XIE, G. M.—MA, Z. Y.—GENG, L.—CHEN, R. S.: *Materials Science and Engineering A*, 71, 2007, p. 63. [doi:10.1016/j.msea.2007.03.041](https://doi.org/10.1016/j.msea.2007.03.041)
- [19] DARRAS, B. M.—KHRAISHEH, M. K.—ABU FARHA, F. K.—OMAR, M. A.: *Journal of Materials Processing Technology*, 191, 2007, p. 77. [doi:10.1016/j.jmatprotec.2007.03.045](https://doi.org/10.1016/j.jmatprotec.2007.03.045)
- [20] LIM, S.—KIM, S.—LEE, C. G.—YIM, C. D.—KIM, S. J.: *Metall. Mater. Trans. A* 36, 2005, p. 1609. [doi:10.1007/s11661-005-0252-7](https://doi.org/10.1007/s11661-005-0252-7)
- [21] PARK, S. H. C.—SATO, Y. S.—OKAWA, H.: *Metall. Mater. Trans. A*, 34, 2003, p. 987. [doi:10.1007/s11661-003-0228-4](https://doi.org/10.1007/s11661-003-0228-4)
- [22] DENQUIN, A.—ALLEHAUX, D.—CAMPAGANC, M. H.—LAPASSET, G.: *Welding in the World*, 46, 2002, p. 14.
- [23] VILACE, P.—QUINTINO, L.—SANTOS, T. F. D.: *J. Mater. Proc. Technol.*, 169, 2005, p. 452.
- [24] LEE, W. B.—YEON, Y. M.—JUNG, S. B.: *Mater. Sci. Technol.*, 19, 2003, p. 785. [doi:10.1179/026708303225001867](https://doi.org/10.1179/026708303225001867)
- [25] NELSON, T.—STEEL, R.—ARBEGAST, W.: *Sci. Technol. Weld. Joining*, 8, 2003, p. 283. [doi:10.1179/136217103225011005](https://doi.org/10.1179/136217103225011005)
- [26] SATO, Y. S.—URATA, M.—KOKAWA, H.—IKEDA, K.: *Mater. Sci. Eng. A*, 354, 2003, p. 298. [doi:10.1016/S0921-5093\(03\)00008-X](https://doi.org/10.1016/S0921-5093(03)00008-X)